

Numerical Simulation of Rejection of Ions in Dilute Solution by LPRO Membrane under Very Low Pressure Operation

Chavalit Ratanatamskul, Kazuo Yamamoto and Shinichiro Ohgaki
Department of Urban Engineering, The University of Tokyo

1. Introduction

The development of LPRO or nanofiltration as thin film composite membranes has provided the possibility to selectively separate various substances under very low operating pressures. Lower pressure operation is very attractive in reducing operational costs. The LPRO membranes used in this research are charged membranes. Therefore, there is a possibility of separating ions according to their valence by the electric repulsion force. Previously, some transport models of charged reverse osmosis membranes have been proposed and separation dependency upon feed concentration, membrane charge density and permeate volume flux has been indicated. However, few reports have experimentally compared the experimental data with the theory. Here, the extended Nernst-Planck model was applied to the analysis of the experimental data of dilute ionic solution under very low pressure operation by considering the effective charge density of the membranes.

2. Transport phenomena equation for charged RO membrane

The extended Nernst-Planck equation proposed by Dresner (1972) is as follows :

$$j_i = -c_i u_i RT \frac{d(\ln a_i)}{dx} - z_i c_i u_i F \left(\frac{d\psi}{dx} \right) - c_i u_i v_i \left(\frac{dP}{dx} \right) + \beta_i c_i j_v \quad (1)$$

The third term in Eq.(1) is mostly negligible. The electroneutrality condition is expressed as:

In external solution:

$$\sum z_i C_i = 0 \quad (2)$$

In membrane:

$$\sum z_i c_i + \Phi X = 0 \quad (3)$$

The Donnan equilibrium at an interface between the membrane and the external solution can be assumed:

$$(\gamma c_i / \gamma_o C_i)^{1/z_i} = \exp(-F/RT \Delta \psi^D) \quad (4)$$

From (1) to (3);
$$d\psi/dx = \frac{\sum (z_i / u_i) (c_i - C_{i,p}) j_v}{F \sum (z_i^2 c_i)} \quad (5)$$

$$dc_i/dx = \frac{(c_i - C_{i,p}) j_v}{u_i RT} - \frac{z_i c_i F (d\psi/dx)}{RT} \quad (6)$$

And $(j_v A k) = A \Delta P \quad (7); \quad R = 1 - C_{i,p}/C_{i,m} \quad (8)$

The calculation can be done by numerically integrating equations from (2) to (8) by Rung-Kutta method.
Nomenclature: j_i = the flux of the i -th ion through the membrane based on membrane pore area; x = membrane thickness; β_i = convective coefficient; c_i = conc. of ion inside the membrane; C_i = conc. of ion in the external solution; z_i = valence of ion; ΦX = effective charge density of membrane; $\Delta \psi^D$ = Donnan potential at the membrane interface; ψ = electric potential; $C_{i,p}$ = effluent conc. of ion in the external solution; j_v = volume flux based on membrane pore area; u_i = molar mobility; v_i = specific volume; P = hydraulic pressure; F = Faraday constant; R = gas constant or rejection; T = temperature; a_i = activity; Ak = surface porosity; γ, γ_o = activity coefficients in membrane and in external solution; ΔP = transmembrane pressure difference; A = permeability coefficient; $C_{i,m}$ = concentration at membrane surface

3. Experimental methods

Two types of membranes used in this research are listed below:

Table 1 Characterization of LPRO membranes used

Membrane Type	Surface Material
NTR-7250	Polyvinyl alcohol
NTR-729HF	Polyvinyl alcohol

The membrane module used here is a flat-sheet type C-10T (Nitto Denko Co.) and effective membrane surface area of the module is 60 cm². The operating pressures used were in the range of 0.05 - 0.39 MPa, which is considerably low pressure range for LPRO-membrane operation. Anion concentrations were measured by the indirect UV method of HPLC (Shimadzu LC-6A). This method utilized IC-A1 column. Phthalic acid of 0.5 mM (pH = 4.6) was used as liquid phase. The detection wavelength of UV is 260 nm.

4. Results and discussion

4.1 Effect of transmembrane pressure on ionic rejection

Figures 1&2 show the relationships between rejection and transmembrane pressure for dilute sodium chloride concentration of 1 mmol/l in the cases of membrane types NTR-7250 and NTR-729HF, respectively. Rejection increases with an increase in transmembrane pressure. It is apparent that the model could fit the experimental data very well even at transmembrane pressure less than 0.1 MPa. Two transport parameters of $\Delta x/Ak$ (membrane thickness / surface porosity) and $\Phi X/C_m$ (effective membrane charge density / influent conc.) obtained here were 1.3×10^{-4} m and 51 in the case of NTR-729HF. They were 9.94×10^{-5} m and 25 in the case of NTR-7250.

4.2 Concentration profiles of ions inside the membrane

Concentration profiles of sodium and chloride ions across the membrane were numerically simulated. It was found that the concentration of chloride ion significantly decreased with the distance inside the membrane. In the case of NTR-7250, it is apparent that when much lower pressure operation of 0.067 MPa or less was employed as shown in Fig.3, more thickness of membrane might be required to reach the same reduction as in the case of higher pressure operation. From Figs 3&4, the approximately 1000 times higher concentration of sodium ion than that of chloride ion inside the membrane is caused by the electric potential occurred inside the membrane. The electric potential here tends to repulse chloride ion, a co-ion for membrane surface charge, from entering inside the membrane. In contrast, the electric potential results in accumulating sodium ion, which is a counter-ion to membrane-surface charge, inside the membrane. Moreover, increasing transmembrane pressure causes an increase in electric potential. Therefore, it yielded in higher concentration of accumulated sodium ion and in higher reduction of chloride ion inside the membrane as shown in Figs.3&4.

4.3 Effect of feed concentration on ionic rejection

The study on the effect of different feed concentration of sodium chloride solution on ionic rejection was done with the membrane type NTR-7250. The data obtained from simulation of the model was also compared with the experimental results as shown in Fig.5. It is apparent that the rejection decreased with increasing the feed concentration under all range of operating pressures applied. This characteristic might be explained by the fact that the Donnan potential for electric repulsion becomes less effective when higher concentration of ions comes through the charged membrane as expressed in Eq.(4). It was found that the model could fit the experimental results well under operating pressures of 0.294 and 0.098 MPa. However, in the case of very much lower operating pressure of 0.059 MPa, the rejection values obtained from the experiment data here were less than the predicted ones by the model for all range of the feed concentration applied. This implies that further improvement for the model under very much low operating condition should be made. When the effective charged density of membranes was plotted against feed concentration as shown in Fig.6, it was found that the estimated effective charged density increases with an increase in feed concentration of ionic solution. This means that higher dissociation of the ionic group on membrane surface was obtained. The reason for this phenomena follows the rule of electroneutrality inside the membrane (Eq.3) that more amounts of sodium ion could come inside when feed solution of higher concentration is applied. Then effective charge density of membrane has to be risen to keep neutral condition inside the membrane.

5. References

- L.Dresner, *Desalination*, 10(1972) 17-26
- T.Tsuru, S.Nakao and S.Kimura, *J. Chemical Eng. of Japan*, 24(1991):4, 511-524

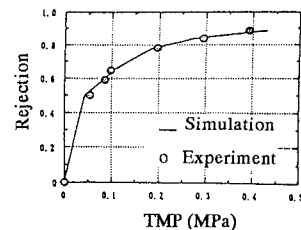
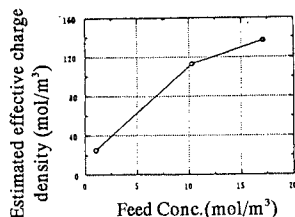


Fig.1 Comparison result for NTR-729HF

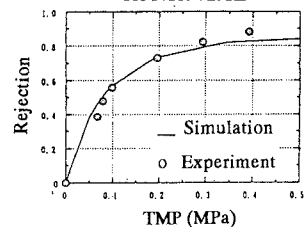


Fig.2 Comparison result for NTR-7250

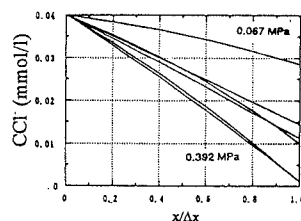


Fig.3 Concentration gradient of Cl⁻ for NTR-7250

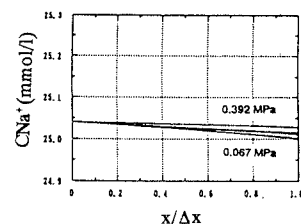


Fig.4 Concentration gradient of Na⁺ for NTR-7250

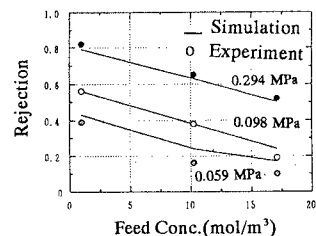


Fig.5 The effect of feed conc. of Cl⁻ on rejection

Fig.6 The estimated effective charge density of membrane with different feed conc. of Cl⁻